NONLINEAR STRUCTURING EFFECTS IN ROTATING AND STABLY STRATIFIED TURBULENT FLOWS

Fabien S. Godeferd & Claude Cambon
LMFA UMR 5509, École Centrale de Lyon,
BP 163, 69131 Ecully, France

INTRODUCTION

The effects of rotation on the structure of weak and developed turbulence present interest in industrial flows, while stable density stratification and coupled stratification-rotation effects occur in geophysical flows. In these cases, the role of body forces (Coriolis, buoyancy) and mean gradients (density but not velocity) is subtle and difficult to model, since their linear dynamics consist of steady or oscillating modes of motion, the latter being linked to dispersive waves. By contrast with shear flows, there is no direct production of energy by linear effects, and the alteration of dynamics is essentially controlled by nonlinear interactions, such as resonant waves for instance. Given the complexity of this general problem, we will restrict the study to the case of homogeneous turbulence, assuming unbounded fluctuating flows — or flows in periodic boxes for DNS realizations — and uniform mean temperature gradient. For this homogeneous, and generally anisotropic, turbulence, the Fourier decomposition leads to analytical solutions for the linear regime, in accordance to "Rapid Distortion Theory" (RDT) and nonlinear dynamics is simulated by pseudo-spectral DNS codes, or modeled by two-point closures. Of course, spectral description includes the exact dispersion law of inertio-gravity waves. RDT and DNS results have been contrasted both in the rotating and in the stratified cases, separately considered. Given the limits of RDT, an original version of the EDQNM theory (Orszag 1970), called EDQNM2, has been extensively exploited to predict the nonlinear interactions in both cases, with quantitative comparisons with DNS (Cambon et al. 1997, Godeferd & Cambon 1994, Staquet & Godeferd 1998). In these previous works was used a projection of the fluctuating velocity/temperature field onto the eigenmodes of the linear regime. Nonlinear interactions were also further analyzed in terms of these eigenmodes. In addition, the whole study has suggested a complete anisotropic description of the second order spectral tensor of double correlations, even for post-processing DNS data, which allows to quantify partial two-dimensionalization or two-componentalization (see below). The angular dependence in spectral space, or accordingly the conical structure of the spectral energy containing region — including the separation into different energy modes —, was shown to be a crucial indicator. Of course, to some extent these indicators are reflected in classical correlations in physical space. Among the latter, the integral length-scales involving different directions are the most significant. Our main purpose is to extend these studies to the coupled rotation+stratification case in order to clarify and to model the interaction of both steady and wavy modes in the long-time dynamics of "pancakes" (layering) or "columnar" (two-dimensionalization) structures. Previous DNS studies are not conclusive, and asymptotic analyses (see Babin et al. 1998) only concern the coupled case in boxes with small aspect ratio.

Although RDT captures a part of the dynamics in particular cases of flows subjected to pure rotation or pure stable stratification, and in the latter case can compare well with DNS results (vanHaren 1993 and Hanazaki & Hunt 1997), such a linear approach gives no insight into the creation of irreversible anisotropy. This creation is connected to two-dimensionalization in rotating turbulence or horizontal layering tendency in the stably stratified case. In other words, RDT dynamics characterizes a phase turbulence which conserves some modes of spectral density of energy: kinetic energy for the rotating case, total energy for the stably stratified case. However, two-dimensionalization or two-componentalization, meaning horizontal layering, which affect the distribution of this energy, are typically nonlinear effects. One illustration is the development of two typical integral length-scales as shown in the following. The blocking of the scale L_{11}^3 which characterizes the vertical coherence of the horizontal field, and the continuous increase of L_{11}^1, which characterizes horizontal coherence, is only obtained in nonlinear calculations (DNS and EDQNM2), but not in RDT. This nonlinear behavior provides the best quantification of the rise of vertical layering in physical space. In the

coupled case with both rotation and stable stratification, the consensus seems not to be complete about the respective roles of linear and nonlinéar terms in building pancake or columnar-type structuring (Kimura, private communication). Previous DNS and LES are not conclusive, since emphasis is given to isovorticity surfaces or spherically averaged spectra, and often the resulting observations are biased by numerical artifacts such as insufficient resolution or interference with periodic boundaries. In order to further investigate linear and nonlinear phenomena, we propose the following strategy. First, background solutions of RDT, which are analytically known for the coupled case (Godeferd 1994, Kimura private communication) are used to calculate the statistical correlations (two-point or one-point) which are relevant for describing the anisotropic structure directly connected to layering or two-dimensionalization. These results will be compared with the results of DNS, in an attempt at providing a more complete answer on what is linear — given by RDT — and what is nonlinear — only given by DNS. In addition to such numerical comparisons which exhibit the typically nonlinear effects, RDT has another role. Not only does it provide the reference for pure linear dynamics, but also the eigenmodes of the linear regime form a useful basis for expanding the fluctuating velocity-temperature field, even when nonlinearity is present. Nonlinear interactions can then be evaluated and discussed in terms of triadic interactions between these eigenmodes. Accordingly, the complete anisotropic description of two-point second order correlations can be related to spectra and cospectra of these eigenmodes.

The Boussinesq equations are considered in a rotating frame. Linear operators involve two frequencies, the Brunt-Wäisälä (BV) frequency N associated with the stable stratification, and the Coriolis parameter 2Ω. Our RDT analytical study uses these equations in Fourier space.

Three cases will be considered in the following: $2\Omega/N \ll 1$, $2\Omega/N = 1$ and $2\Omega/N \gg 1$.

THE LINEAR APPROXIMATION

Normal Modes Background For Linear Solutions

We use here the same notations as in Godeferd and Cambon (1994). The fluctuating fields for velocity $\boldsymbol{u}$ and temperature τ are gathered into a unique three-dimensional vector $\boldsymbol{v}$. The Fourier coefficients for its 3 components in the fixed frame of reference are $(v_i, i = 1,2,3)$, with 3 the vertical direction. They become ϕ^i in the Craya-Herring local frame $(\boldsymbol{e}^1, \boldsymbol{e}^2, \boldsymbol{e}^3 = \boldsymbol{k}/k)$. The unit vectors $\boldsymbol{e}^1$ and $\boldsymbol{e}^2$ lie in the plane orthogonal to $\boldsymbol{k}$, such that $\boldsymbol{e}^1$ is horizontal. Greek superscripts only take the values 1 or 2, so that ϕ^α refers to the fluctuating velocity field components in the local frame, and a kinematically rescaled fluctuating temperature Fourier component is used: $\phi^3 = \mathrm{i}(\beta g/N)\widehat{\tau}$. The linearized system of equations in the Craya-Herring frame becomes

$$\begin{pmatrix} \dot{\phi}^1 \\ \dot{\phi}^2 \\ \dot{\phi}^3 \end{pmatrix} + \begin{pmatrix} 0 & -\sigma_r & 0 \\ \sigma_r & 0 & \sigma_s \\ 0 & -\sigma_s & 0 \end{pmatrix} \begin{pmatrix} \phi^1 \\ \phi^2 \\ \phi^3 \end{pmatrix} = \mathbf{0} \qquad (1)$$

or $\dot{\boldsymbol{\phi}} + \mathbf{M}\boldsymbol{\phi} = \mathbf{0}$, where $\sigma_r = 2\Omega\cos\theta$, $\sigma_s = N\sin\theta$, $\sigma = \sqrt{\sigma_r^2 + \sigma_s^2}$ are respectively the absolute value of dispersion law frequencies for inertial waves, gravity waves and inertio-gravity waves. The system of equations (1) is easily solved by diagonalizing the matrix $\mathbf{M}$. The three following eigenmodes are obtained in the local frame:

$$\boldsymbol{N}^0 = \begin{pmatrix} -\sigma_s/\sigma \\ 0 \\ \sigma_r/\sigma \end{pmatrix}, \quad \boldsymbol{N}^{\pm 1} = \frac{\sqrt{2}}{2} \begin{pmatrix} \sigma_r/\sigma \\ \mp\mathrm{i} \\ \sigma_s/\sigma \end{pmatrix} \qquad (2)$$

respectively related to the eigenvalues 0 and the two $\pm\sigma$. $\mathbf{N}^0$ is the stationary mode, which coincides with the quasi-geostrophic mode (QG). It comprises two contributions, one from the horizontal divergence-free velocity mode ϕ^1 ('vortex' mode), and one from the mode ϕ^3 associated with the temperature field. The wavy modes are $\mathbf{N}^{\pm 1}$, also called ageostrophic modes (AG) hereinafter in agreement with classic geophysical literature. Note that the latter wave-affected modes, setting either $N = 0$ in (2) or $\Omega = 0$ depending on the case, do not exactly coincide with the corresponding modes that were defined in the particular cases of pure rotation (Cambon et al., 1997) or pure stratification (Godeferd & Cambon, 1994). The difference arises from different normalization coefficients (namely i, $-\mathrm{i}$, $\sqrt{2}$). The wave/vortex terminology was used by Riley et al. (1981) for the analysis of DNS of stably stratified turbulence, and in a more geophysically related context, the geostrophic and ageostrophic counterparts, by Bartello (1995) and Babin et al. (1998).

The basis of eigenmodes is used to express $\boldsymbol{v}$ as

$$\boldsymbol{v} = \sum_{\epsilon=0,\pm 1} \xi^\epsilon \boldsymbol{N}^\epsilon \,, \qquad (3)$$

$$\xi^\epsilon = \boldsymbol{v} \cdot \boldsymbol{N}^{-\epsilon}, \quad \epsilon = 0, \pm 1 \,, \qquad (4)$$

using orthonormal properties of the eigenvectors. Accordingly, the initial value linear problem (1) has a general solution

$$\boldsymbol{v}(\boldsymbol{k}, t) = \sum_{\epsilon=0,\pm 1} \boldsymbol{N}^\epsilon e^{-\mathrm{i}\epsilon\sigma t} \left(\boldsymbol{N}^{-\epsilon} \cdot \boldsymbol{v}(\boldsymbol{k}, t_0 = 0)\right) \,. \qquad (5)$$

RDT Solutions For Second-Order Statistics

From eq. (5), the RDT solutions for any statistical Eulerian quantity may be derived. Second order statistics are given by

$$< v_i^*(\boldsymbol{p}, t) v_j(\boldsymbol{k}, t) >= V_{ij}(\boldsymbol{k}, t)\delta(\boldsymbol{k} - \boldsymbol{p}) \qquad (6)$$

and the RDT equations for V_{ij} are unchanged if one accepts the notation misuse $V_{ij} =< v_i^* v_j >$ for linking V_{ij}

to its initial value through the general solution (5). It then is possible to project two-point statistics onto the local frame, yielding $\Phi^{nm} = e_i^n V_{ij} e_j^m$, as used previously by Godeferd & Cambon (1994), so that Φ^{11}, Φ^{22}, Φ^{33} and Φ^{23} are respectively related to the vortex mode kinetic energy, the wave kinetic energy, the potential energy and the heat flux. The latter also contains the vertical buoyancy flux, an essential quantity of interest in the case of pure stratification. These quantities could be used again in the general rotating and stratified case, but they are less informative, and it is probably sounder to employ the quadratic terms $\xi^{\epsilon *}\xi^{\epsilon'}$ related to the QG and AG eigenmodes, since they lead to an exact tensorial diagonalisation. Without any calculation, it is obvious that the RDT temporal evolution of any two-point or one-point correlation can be obtained in a quasi-analytical way provided initial data have simple two-point statistics. For instance, initial three-dimensional isotropy with vertical mirror symmetry yields

$$\Phi^{11} = \Phi^{22} = \frac{Ec(k)}{8\pi k^2}, \quad \Phi^{33} = \frac{Ep(k)}{8\pi k^2}, \qquad (7)$$

all other cospectra being zero. For further simplification, the spherically averaged potential energy spectrum is chosen proportional to the kinetic one, as $Ep = \alpha Ec$.

In the following RDT results, we shall take advantage of two conservation laws. First, total energy is conserved in any orthonormal frame of reference:

$$v_i^* v_j = \phi^{i*}\phi^j = \sum_{\epsilon=0,\pm 1} \xi^{\epsilon *}\xi^{\epsilon} \ .$$

Second, owing to the linear approximation, there is conservation of QG energy, written as $\xi^{0*}\xi^0$ using eq.(2) and (4). Finally since the vertical kinetic and potential energies are contained in $v_3^* v_3$, the horizontal kinetic energy is obtained by difference from total kinetic energy.

Let us point out that for easing the algebra, it is worthwhile to distinguish statistical quantities which only involve an integration in the horizontal wave-plane $k_3 = 0$ from those that require integrating over all k orientations.

Vertically Separated Integral Length Scales. In agreement with the previous definitions, conservation laws and remarks, the following are found with no extra effort. The conservation of $v_i^* v_i$ and integration over the plane $k_3 = 0$ yield

$$\begin{aligned} &< u_1^2 > L_{11}^3 + < u_2^2 > L_{22}^3 + < u_3^2 > L_{33}^3 \\ &+(\beta g/N) < \tau^2 > L_\tau^3 = q_0^2 L_0 (2/3 + \alpha/3) \end{aligned} \qquad (8)$$

where L_0 is the initial integral length scale, proportional to $\int_0^\infty (Ec(k)/k)dk$, and L_τ^3 is defined from the spectrum of potential energy, as are the other L_{ii}^k kinetic lengthscales. From the definition of ξ^0, in terms of $\boldsymbol{N}^0$, using $k_3 = 0$ one computes the horizontal kinetic energy density $\xi^{0*}\xi^0|_{k_3=0} = \phi^{1*}\phi^1$, whereupon integrating yields

$$< u_1^2 > L_{11}^{(3)} + < u_2^2 > L_{22}^{(3)} = q_0^2 L_0/3 \ . \qquad (9)$$

Finally, $< u_3^2 > L_{33}^{(3)}$ and $(\beta g/N) < \tau^2 > L_\tau^{(3)}$ display simple oscillations with opposite phases whereas their sum is constant, as is the case in pure stratification. Notice that both remain constant if there is initial equipartition $\alpha = 1$.

Other Correlations. From the conservation of energy it is found

$$\begin{aligned} &< u_1^2 > + < u_2^2 > + < u_3^2 > \\ &+(\beta g/N)^2 < \tau^2 > = q_0^2 (1 + \alpha/2) \end{aligned} \qquad (10)$$

$$\begin{aligned} &< u_1^2 > L_{11}^1 + < u_2^2 > L_{22}^1 + < u_3^2 > L_{33}^1 \\ &+(\beta g/N) < \tau^2 > L_\tau^1 = q_0^2 L_0 (2/3 + \alpha/3) \ . \end{aligned} \qquad (11)$$

$< u_3^2 >$, $< \tau^2 >$ and $< u_3^2 L_{33}^1 >$ are given by integrals over θ, the angle of $\boldsymbol{k}$ to the vertical. Their history shows damped oscillations due to the integration of $e^{mi\sigma t}$, $m = \pm 1, \pm 2$, and constant terms, corresponding to $m = 0$, due to contributions from $\xi^{0*}\xi^0$, $\xi^{1*}\xi^1$ and $\xi^{-1*}\xi^{-1}$. Hence, analytical estimates are obtained at least for the asymptotic values. Of course, other simplifications due to semi-axisymmetry — axisymmetry without mirror symmetry — need be used. In so doing, we can complement our set of RDT formulas with

$$< u_3^2 > L_{33}^3 = \frac{q_0^2 L_0}{6} \left(1 + \alpha + (1 - \alpha)\cos(2Nt)\right) \qquad (12)$$

$$< u_3^2 > = \frac{q_0^2}{3} \left(C + (1 - \alpha) f(Nt, B)\right) \ , \qquad (13)$$

$$\begin{aligned} C = \frac{3}{4} \int_0^1 &\frac{1 - x^2}{4\Omega^2 x^2 + N^2(1 - x^2)} \\ &\times \left(8\Omega^2 x^2 + N^2(1 - x^2)(1 + \alpha)\right) dx \end{aligned} \qquad (14)$$

$$\begin{aligned} f(Nt, B) = \frac{3}{4} N^2 \int_0^1 &\frac{(1 - x^2)^2}{4\Omega^2 x^2 + N^2(1 - x^2)} \\ &\times \cos\left(2\sqrt{4\Omega^2 x^2 + N^2(1 - x^2)}\, t\right) dx \end{aligned} \qquad (15)$$

The part C depends on parameters α and $B = 2\Omega/N$. It is easy to calculate in the non rotating case $B = 0$, amounting to $C = (1 + \alpha)/2$, and in the non dispersive case $B = 1$ that gives $C = (3 + 2\alpha)/5$. The time-dependent part $f(Nt, B)$ can be shown to give damped oscillations (see fig. 1), but for $B = 1$ for which there is no damping. Using exactly the same mathematical ways, one also shows that

$$\left(\frac{\beta g}{N}\right)^2 < \tau^2 > L_\tau^3 = \frac{q_0^2 L_0}{6} \left(1 + \alpha - (1 - \alpha)\cos(2Nt)\right)$$

in phase opposition of relation (12) as expected.

FULL TURBULENT SIMULATIONS

Numerical method and parameters

We perform Direct Numerical Simulations (DNS) of the previously mentioned Boussinesq equations with Coriolis effect, in a periodic three-dimensional cubic box of size 4π. The method is a standard pseudo-spectral one in Fourier space, with full de-aliasing. The time scheme of third order Adams-Bashforth type. The code has been used by Staquet & Godeferd (1998) in the stably stratified case only, to which we have added the Coriolis term $2\boldsymbol{\Omega} \times \boldsymbol{u}$. The resolution is 128^3, and an isotropic precomputation stage is used for allowing an initially random field to develop a realistic dynamics, before the application of the external gravity and rotation effects, at $t = 0$, say. Therefore, simulations are initiated with zero potential energy, corresponding to $\alpha = 0$. Viscous RDT is obtained by cancelling the nonlinear terms in the DNS code.

Numerical values for the parameters are as follows: in run C30, $2\Omega = N = \pi/2$; in run C3A, $N = 5\pi$, $2\Omega = \pi/2$; run C3B: $N = \pi/2$ and $2\Omega = 5\pi$. The non dimensional parameters are computed at the beginning ($t = 0$); they include the Reynolds number $\mathrm{Re} = q_0 L_0/\nu$, the Rossby number $\mathrm{Ro} = q_0/(2\Omega L_0)$ and the Froude number $\mathrm{Fr} = q_0/(NL)$. Small values of these last two quantities indicate very strong body forces compared with the turbulent momentum transport, or equivalently, dominant linear vs. nonlinear terms. All runs start at rather low $\mathrm{Re} = 100$, due to the initial isotropic precomputation decay. The Froude and Rossby numbers alternately take values of 0.93 (small stratification or rotation) and 0.093 (strong stratification and fast rotation).

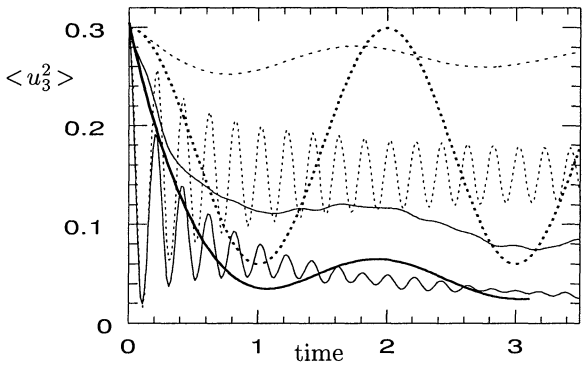

Figure 1: Time plot of $<u_3^2>$: solid lines for DNS results, dotted lines for the analytical prediction of eq. (13). Rapidly oscillating curves for case C3A. Heavy lines represent case C30. Others for C3B.

Results

We shall not dwell on the inhibiting effect upon turbulent energy decay due to either rotation or stratification, since extensive work was devoted to this by Cambon et. al (1997) and Staquet & Godeferd (1998). The purpose of our work is to examine closely the generation of anisotropy due to wave effects, of either linear or nonlinear character.

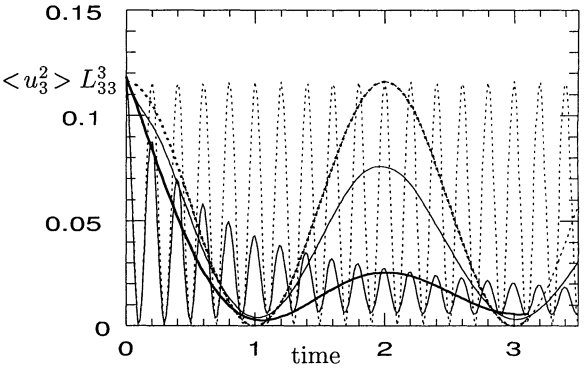

Figure 2: Time plot of $< u_3^2 > L_{33}^3$. Same legend as fig. (1). Analytical results from eq. (12) this time. The analytical curves for cases C30 and C3B are superimposed since the same N is used.

Effects captured by the linear equations. Obviously, the analytical expressions given in the second section are expected to reproduce most of the large scale oscillating effects, which are essentially due to linear terms in the equations: the oscillations of the heat flux are produced by the buoyancy force, and some large scale oscillating motion may be created by the action of the Coriolis term onto the larger structures of the flow. However, it is important to underline that analytical derivations may only be completely carried out in the non viscous case, for which no wavenumber dependent decay occurs. On the contrary, in the viscous case details of the spectral energy distribution plays a role, not only its integral. Indeed, viscous decay occurs at a different rate $exp(-\nu kt)$, thus explicit integration is not possible without the help of numerical tools.

Having said so, we proceed to comparing the time evolution of some quantities predicted in the linear non viscous approximation or computed by DNS. Fig. 1 shows $< u_3^2 >$, proportional to the vertical kinetic energy. As expected, in the strongly stratified case C3A we see that rapid oscillations of $< u_3^2 >$ occur, at a frequency close to the BV frequency $N/2\pi$. For the non dispersive case C30 and the fast rotating one C3B, the oscillating period is much larger, and quite close in the two cases, also driven by the BV frequency. As mentioned, the DNS curves exhibit a temporal decay. If we put this decrease aside, we observe a very good agreement of the oscillation period in the linear results. Such an agreement may be put on the account of our zero potential energy initial conditions. More generally, if kinetic and potential

energies are initially different, large oscillations are generated by gravity, appearing as a linear effect. Otherwise, linear theory concludes to no energy exchange at all in the early decay stage (Staquet & Godeferd 1998). Note also on fig. 1 the analytically predicted damping of the oscillations. Fig. 2 shows the product $< u_3^2 L_{33}^3 >$ which, from eq. (12) is expected to exhibit no damping in its oscillations. Here again the eigen frequency given by linear theory is extremely close to the oscillating frequency computed in the DNS runs. Fig. 3 shows the evolution of the directional length scales for different correlations. In this axisymmetric geometry, one distinguishes mainly correlations of horizontal velocity components in the horizontal or vertical directions, and correlations of the vertical velocity component. Note that correlations parallel to the component considered are twice the others, in isotropic turbulence, whence a dividing "2" coefficient. The dashed curves on this figure represent $L_{33}^3/2$ computed from eq. (12) and (13). Here again, the oscillations are very well tuned with those in DNS for the same quantity. Even the *amplitudes* of these oscillations are observed to be in quite good agreement. The viscous

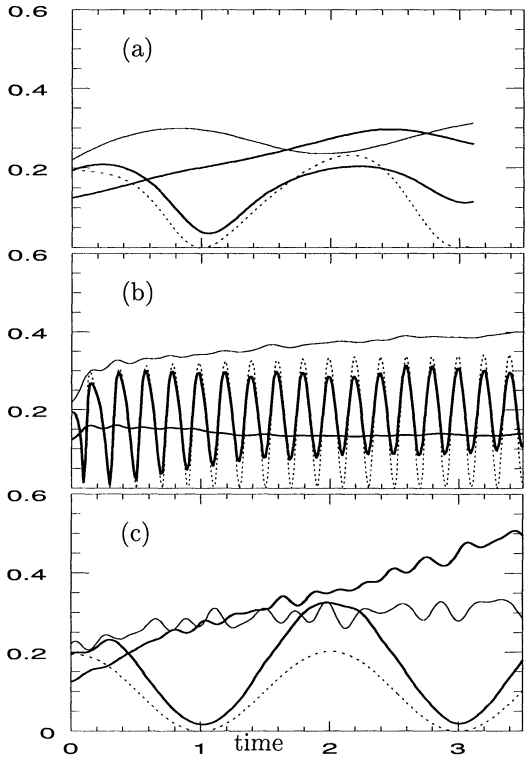

Figure 3: Time evolution of the length scales for: (a) run C30; (c) run C3B; (b) run C3A. —— for the horizontal length scale $(L_{11}^1 + L_{22}^2)/4$. $- -$, $L_{33}^3/2$ computed from eq. (12) and (13). Heavy solid line with largest oscillations: $L_{33}^3/2$ from DNS. The last one is L_{11}^3.

RDT results on fig. 4 show a very good agreement with DNS for the evolution of the horizontal length scale L_h, computed as a mean between L_{11}^1 and L_{22}^2 owing to axisymmetry. The growth of this scale reflects the decay of turbulence, much as in isotropic turbulence, during which total energy is dissipated, and the large energy containing scales are shifted towards smaller wavenumbers. The phase agreement that can be observed comes from the fact that exactly the same velocity/temperature fields are used as initial conditions for both the RDT and DNS runs. (Ideally, some phase-related fluctuations ought to be removed by averaging over a series of different realisations with different initial random distributions.)

What is NOT reproduced by linear approximations. Observing fig. 4, the reader has already noticed that, although the *horizontal* structure of the flow seems to be statistically equivalent in RDT and DNS fields, the *vertical* one appears much different. Indeed, fig. 4 also shows the time evolution of the very important length scale L_{11}^3 (which is actually computed as $(L_{11}^3 + L_{22}^3)/2$). In isotropic turbulence, this length scale should grow exactly in parallel with the horizontal L_h one. On the contrary, the effects of rotation and stratification, both acting in the preferential vertical direction, modify strongly the dynamics of the flow in this direction, whence a different vertical structure as well. For run C3A, stratification appears to dominate, since the layering of the flow is indicated by a very strong vertical decorrelation of horizontal velocity components: not only does L_{11}^3 not grow anymore, but it even decreases slightly. If one adds to that the growth of L_h, we can picture structures in the flow as being "pancake-shaped". A transposed effect is obtained in case C3B, for which the fast rotation rate creates vertically elongated structures, as demonstrated by the large increase of L_{11}^3 on fig. 4, much sharper than that of L_h. [No tendency of one kind or the other is observed for the non-dispersive case C30, for which the inertio-gravity waves do not lead to such clear anisotropic features (see fig. 3(a)).] For both cases, we observe that the linear approximation fails totally in reproducing such a structural tendency. Accordingly, RDT's L_{11}^3 quietly grows as if turbulence were merely in a state of isotropic decay. This demonstrates that a thorough characterization of the structure of turbulence has to be used in such rotating/stratified contexts, for exhibiting the discrepancy between the linear or the full nonlinear modelling approaches.

Finally, we present the spectral characterization of the flow statistics on fig. 5. Of course, the shown *anisotropic* spectra contain the same information as the correlation integral length, and more. We present the total energy density spectra, accumulated in three sub-domains of spectral space: the conical polar sector with wavevectors close to the vertical direction, the equatorial sector with almost horizontal wavevectors, and the intermediate one. As plotted, the layering of the flow for case

C3A translates into much more energy being contained in the polar region. On the contrary, for case C3B, more energy is accumulated in the equatorial direction. The spectral analysis deserves a long discussion, but our point here is to show this strong angular dependence of the anisotropic spectra generated by DNS. However, the lack of "coherence" of the kinematically evolving fields in the linear approximation conserves the exact isotropy of the energy spectrum simulated by viscous RDT, as shown in the small sub-plot of fig. 5. We conclude that irreversible anisotropy, as in the spectra of fig. 5, is unattainable by simple linear RDT assumptions.

Acknowledgements. Calculations have been performed on the Cray C98 of IDRIS (CNRS), thanks to computed time allocated by the Scientific Council of IDRIS.

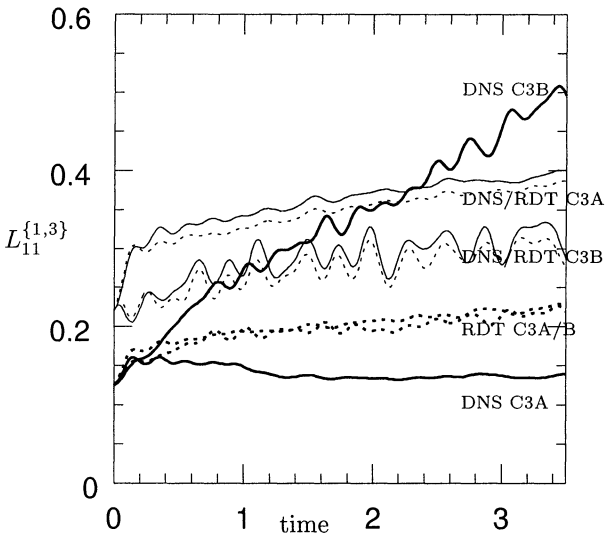

Figure 4: Time evolution of the directional length scales in the DNS (solid lines) and the viscous RDT (dashed lines) runs C3B and C3A. Heavy lines for L_{11}^3, thin lines for $(L_{11}^1 + L_{22}^2)/4$.

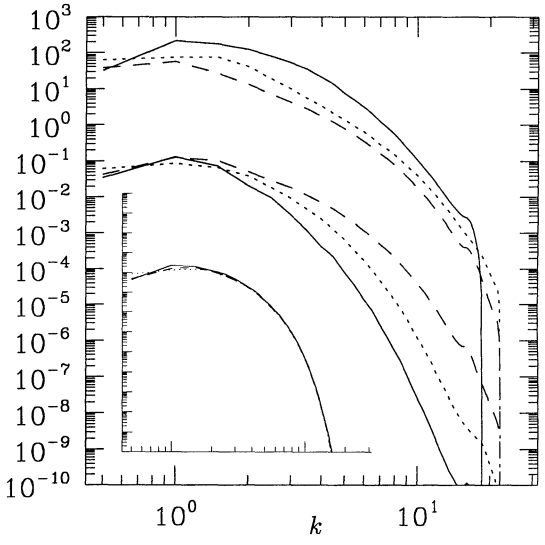

Figure 5: Total energy anisotropic spectra: ——, polar direction; · · · ·, intermediate direction; — —, equatorial direction. Top curves for case C3A, at end of run, shifted three decades up. Three bottom curves for case C3B at the end of the run. The encapsulated plot shows the same for the C3B RDT run. Spectra in the C3A RDT case are almost indistinguishable from these. (Reduced scale, but otherwise same ranges.)

References

Babin, A., Mahalov, A., and Nicolaenko, B., 1998, *Theor. Comput. Fluid Dynamics*, Vol. 11, pp. 215-235.

Bartello, P., 1995, "Geostrophic adjustment and inverse cascades in rotating stratified turbulence," *J. Atmos. Sci.*, Vol. 52, pp 4410-4428.

Cambon, C., Mansour, N.N., and Godeferd, F.S., 1997, "Energy transfer in rotating turbulence," *J. Fluid Mech.*, Vol. 337, pp. 303-332.

Cambon, C., and Scott, J.F., 1998, "Linear and nonlinear models of anisotropic turbulence," *Ann. Rev. Fluid Mech.*, Vol. 61, pp. 1-53.

Godeferd, F.S. 1994, "Introduction d'une partition ondes-turbulence dans les modèles de transport pour les écoulements turbulents stablement stratifiés," PhD thesis, École Centrale de Lyon.

Godeferd, F.S., and Cambon, C., 1994, "Detailed investigation of energy transfers in homogeneous turbulence," *Phys. Fluid*, Vol. 6, pp. 2084-2100.

Hanazaki, H., and Hunt, J.C.R, 1996, "Linear processes in unsteady stably stratified turbulence," *J. Fluid Mech.*, Vol. 318, pp. 303-337.

Riley, J.J., Metcalfe, R., and Weissman, M.A., 1981, "Direct numerical simulations of homogeneous turbulence in density-stratified fluids," *Advances in Turbulence*, Springer, pp. 184-190.

Smith, L., and Waleffe, F., 1998, "Transfer of energy to 2D large scales in forced, rotating 2D turbulence," *Phys. Fluid*, submitted.

Staquet, C., and Godeferd, F.S., 1998, "Statistical modeling and direct numerical simulations of decaying stably stratified turbulence. Part 1. Flow energetics," *J. Fluid Mech.*, Vol. 360, pp. 295-240.

VanHaren, L., 1993, "Étude théorique et modélisation de la turbulence en présence d'ondes internes," *PhD thesis*, École Centrale de Lyon.

Zakharov, V.E., L'vov, V.S., and Falkowich, G., 1992, *Kolmogorov spectra of turbulence. I. Wave turbulence*, Springer series in nonlinear dynamics, Springer Verlag.